Highly Nonproductive Complexes with *Anabaena* Ferredoxin at Low Ionic Strength Are Induced by Nonconservative Amino Acid Substitutions at Glu139 in *Anabaena* Ferredoxin:NADP$^+$ Reductase†

John K. Hurley,‡ Merche Faro,§ Tammy B. Brodie,‡ James T. Hazzard,‡ Milagros Medina,§ Carlos Gómez-Moreno,§ and Gordon Tollin*,‡

Department of Biochemistry, University of Arizona, Tucson, Arizona 85721, and Departmento de Bioquímica y Biología Molecular y Celular, Universidad de Zaragoza, 50009 Zaragoza, Spain

Received May 17, 2000; Revised Manuscript Received August 3, 2000

ABSTRACT: Ferredoxin (Fd) and ferredoxin:NADP$^+$ reductase (FNR) from *Anabaena* function in photosynthetic electron transfer (et). The et interaction between the FNR charge-reversal mutant E139K and Fd at 12 mM ionic strength (μ) is extremely impaired relative to the reaction with wt FNR, and the dependency of k_{obs} on E139K concentration shows strong upward curvature at protein concentrations $\geq$10 μM. However, at values of $\mu \geq 200$ mM, reaction rates approach those of wild-type FNR, and normal saturation kinetics are observed. For the E139Q mutant, which is also significantly impaired in its et interaction with Fd at low FNR concentrations and low μ values, the dependency of k_{obs} on E139Q concentration shows a smaller degree of upward curvature at $\mu = 12$ and 100 mM and shows saturation kinetics at higher values of μ. wt FNR and the E139D mutant both show a slight amount of upward curvature at FNR concentrations >30 μM at $\mu = 12$ mM but show the expected saturation kinetics at higher values of μ. These results are expained by a mechanism in which the mutual orientation of the proteins in the complex formed at low ionic strength with the E139K mutant is so far from optimal that it is almost unreactive. At increased E139K concentrations, the added mutant FNR reacts via a collisional interaction with the reduced Fd present in the unreactive complex. The et reactivity of the low ionic strength complexes depends on the particular amino acid substitution, which via electrostatic interactions alters the specific geometry of the interface between the two proteins. The presence of a negative charge at position 139 of FNR allows the most optimal orientations for et at ionic strengths below 200 mM.

There are numerous electron-transfer (et)[1] systems found throughout biology whose function depends on the recognition and proper interaction between proteins that shuttle electrons along these pathways. Photosynthetic et, in a reaction driven by light energy, removes electrons from H_2O and ultimately uses these to reduce CO_2 to carbohydrate. There are a number of membrane-associated and soluble redox proteins involved in the photosynthetic apparatus of plants, algae, and oxygenic photosynthetic bacteria (such as the cyanobacterium *Anabaena*). Two of these soluble et proteins, ferredoxin (Fd) and ferredoxin:NADP$^+$ reductase (FNR), have been the subject of numerous studies in the authors' laboratories, using a combination of site-directed mutagenesis and laser flash photoloysis/transient absorbance measurements to evaluate the relative importance of a large number of surface amino acid residues involved in the interaction of these two proteins.

Fd from vegetative cells of *Anabaena* 7120 is an 11-kDa protein containing one [2Fe-2S] cluster. FNR from the closely related *Anabaena* 7119 is a 36-kDa protein containing a noncovalently bound FAD cofactor. Fd (*1*, *2*) and FNR (*3*−*5*) have both been cloned and overexpressed in *Escherichia coli*, and high-resolution X-ray crystal structures are available for both proteins (*6*−*8*). For these reasons, this protein pair is an ideal system to study structure−function relationships in et proteins. Fd, the ultimate electron acceptor from photosystem I, transfers two electrons in two one-electron steps to FNR. FNR then catalyzes the 2-electron reduction of NADP$^+$ to NADPH (eq 1):

$$2Fd_{red} + NADP^+ + H^+ \rightarrow 2Fd_{ox} + NADPH \quad (1)$$

Kinetic measurements (*9*−*13*) of the reduction of oxidized FNR (FNR_{ox}) by reduced Fd (Fd_{red}) are consistent with a minimal two-step mechanism involving formation of an intermediate complex followed by intracomplex et, as depicted in eq 2:

$$Fd_{red} + FNR_{ox} \overset{K_d}{\rightleftharpoons} [Fd_{red}\text{- - -}FNR_{ox}] \xrightarrow{k_{et}} Fd_{ox} + FNR_{red} \quad (2)$$

† This research was supported by grants from the National Institutes of Health (DK15057 to G.T.) and from the Comisión Interministerial de Ciencia y Tecnología (BIO97-0912CO2-01 to C.G.-M.).

* To whom correspondence should be addressed. E-mail: gtollin@u.arizona.edu. Fax: (520)621-9288.

§ Universidad de Zaragoza.

‡ University of Arizona.

[1] Abbreviations: dRf, 5-deazariboflavin; et, electron transfer; Fd, ferredoxin; Fd_{ox}, oxidized ferredoxin; Fd_{red}, reduced ferredoxin; FNR, ferredoxin:NADP$^+$ reductase; FNR_{ox}, oxidized ferredoxin:NADP$^+$ reductase; FNR_{red}, reduced ferredoxin:NADP$^+$ reductase; μ, ionic strength; wt, wild type.

10.1021/bi001124r CCC: $19.00
Published on Web 10/21/2000

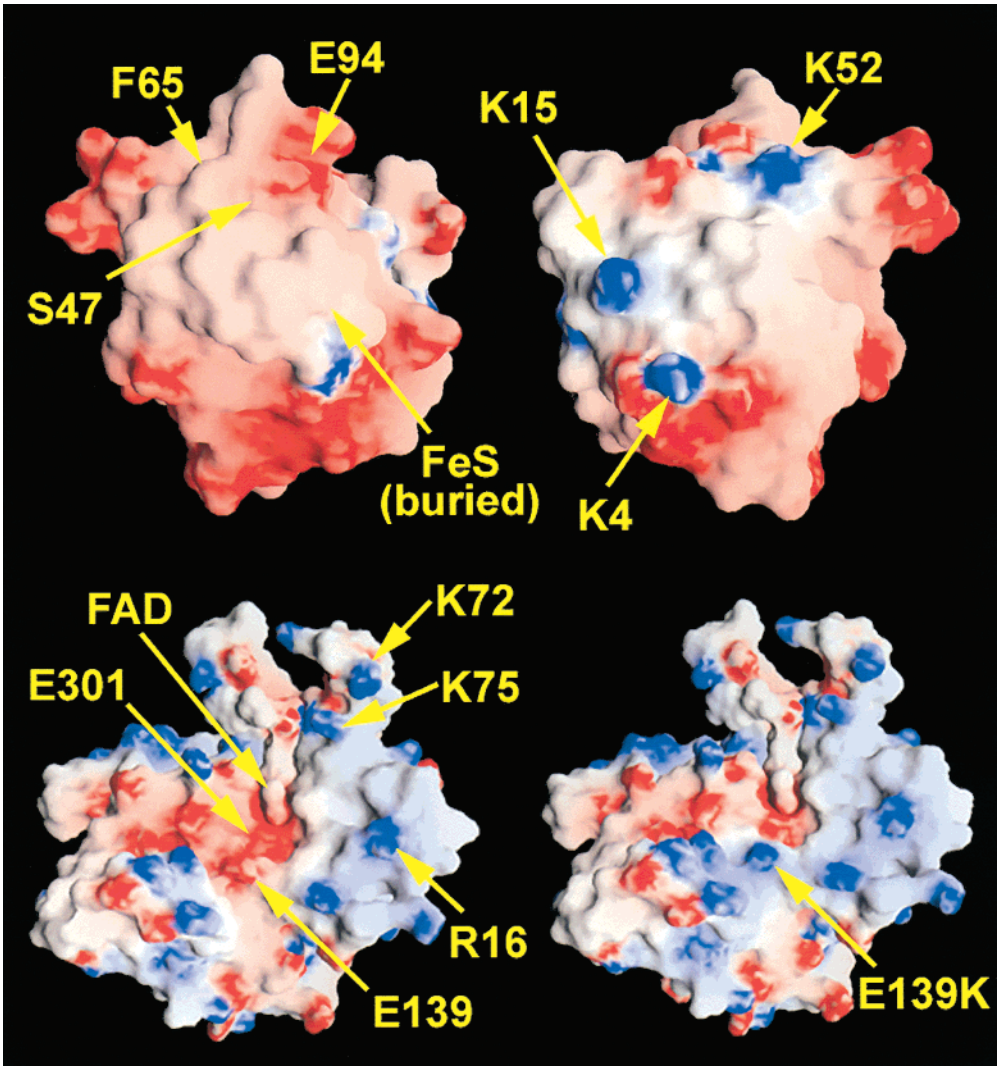

FIGURE 1: Molecular models of Fd (upper) and FNR (lower) showing electrostatic surface potentials mapped onto their surfaces as described in the text. The model shown in the upper left represents the front side of Fd, and the model in the upper right shows a 180° rotation about the *y*-axis. wt FNR is shown in the lower left, and the E139K FNR muant is shown in the lower right. Positive potential is shown in blue, and negative potential is shown in red. Mutated residues discussed in the text and the [2Fe-2S] and FAD cofactors of Fd and FNR, respectively, are labeled.

In such experiments, values for K_d and k_{et} can be determined by fitting the kinetic data to the exact solution for the differential equations describing this mechanism (*14*, *15*).

In previous work from these laboratories, we have shown the requirement in Fd for an aromatic amino acid at position 65 (*10*, *16*; see the electrostatic potential maps shown in Figure 1 for the location of this residue and of those residues in Fd and FNR discussed below), an acidic amino acid residue at position 94 (*10*, *17*), and an amino acid bearing a hydroxylated side chain at position 47 (*11*) in order for efficient et to FNR to proceed (see ref *18* for an overview of structure−function studies of *Anabaena* Fd). The crucial role of the S47 residue has been discussed in light of the recent X-ray structure determination (*19*) of the oxidized and reduced forms of Fd from the closely related *Anabaena* 7119. This study confirmed the central role of the Ser47 hydroxyl group as a major stabilizing factor of the molecular surface. The principal difference between the oxidized and reduced crystals involved the peptide bond joining Cys46 and Ser47. In the oxidized crystals, the Cys46 carbonyl oxygen points toward the [2Fe-2S] cluster and points away from the cluster in the reduced crystals. The authors suggest that this "flip" of the Cys46 carbonyl may be the signature of the reduction of the iron atom (Fe1).

It has also been demonstrated for FNR that a positively charged amino acid is required at position 75 (*20*, *21*) and that K72 (*21*) and R16 (*21*) are also critical residues for efficient et. This has been confirmed by steady-state $NADP^+$ photoreduction assays (*22*). In addition, E301 of FNR has been shown to be a crucial residue for the catalytic functions of the enzyme (*23*), and an X-ray structure has been determined for the E301A FNR mutant (*24*). The crystal structure of this mutant shows greater solvent exposure of the dimethylbenzene ring of the FAD cofactor, which may facilitate access of oxygen to the reduced FAD. The authors suggest this difference as a possible reason for the production of H_2O_2 by this mutant (*23*) upon oxidation by O_2, rather than $O_2^{\bullet-}$, which is produced in the case of wt FNR. E301 has also been shown to stabilize the semiquinone form of the FAD cofactor (*23*).

The present study demonstrates the critical nature of the negative charge at position 139 in FNR for efficient et with Fd. Furthermore, it is shown that, for the E139K mutant at low ionic strength, the complex formed between the mutant

FNR_{ox} and Fd_{red} reacts so slowly that the complexed Fd_{red} is able to react with another FNR_{ox} molecule in a collisional interaction to yield FNR_{red} and Fd_{ox}. It is also shown that similar interactions may be a general phenomenon for protein pairs at low ionic strengths when complexation results in nonoptimal orientations for et, i.e., orientations that cause the cofactors to "communicate" less efficiently. Such reactions involving et proteins are not unique and have been described previously for the cytochrome *c*:cytochrome *c* peroxidase system (*25*−*29*).

MATERIALS AND METHODS

Protein Preparation. Recombinant wt Fd was prepared as described previously (*10*). Recombinant wt and mutant FNRs were prepared from IPTG-induced cultures also as previously described (*23*, *30*). FNR concentrations were determined spectrophotometrically using an extinction coefficient of 9400 M^{-1} cm^{-1} at 459 nm (*31*). Fd concentrations were determined using an extinction coefficient of 9700 M^{-1} cm^{-1} at 422 nm (*32*). Spectra were recorded using either an Olis-modified Cary-15 spectrophotometer or a Hewlett-Packard 8453 diode array spectrophotometer.

Mutagenesis. Site-directed FNR mutants were made using the Transformer mutagenesis kit (Clonetech, Palo Alto, CA), which is based on the unique site elimination method of Deng and Nickoloff (*33*). Mutagenic primers used were as follows: 5′-GG TAA CAG CAT *GTC* TTT ACC CAG AGG-3′ for E139D, 5′-GG TAA CAG CAT *CTG* TTT ACC CAG AGG-3′ for E139Q, and 5′-GG TAA CAG CAT *TTT* TTT ACC CAC AGG-5′ for E139K. Base changes are italicized. The sequence of the selection primer, which converts an *Nde*I restriction site to a *Sac*II site, was 5′-AGT GCA CCA TCC GCG GTG TGA-3′. Primers were synthesized commercially by Sigma Genosys (The Woodlands, TX). Mutations were verified by DNA sequence analysis. Molecular biology procedures followed standard protocols (*34*, *35*).

Laser Flash Photolysis/Transient Absorbance Measurements. The laser and associated optics used for obtaining transient kinetic traces initiated by laser flash photolysis have been described (*36*, *37*), except that a Tektronix TDS 410A digitizing oscilloscope was used in the current apparatus. The photochemical mechanism by which 5-deazariboflavin (dRf) initiates et has also been described (*38*−*40*). Briefly, the triplet excited state of dRf, generated by a laser flash, extracts a hydrogen atom from EDTA to generate the highly reducing dRf semiquinone radical (dRfH$^{\bullet}$) which, in competition with its own disproportionation, reduces Fd_{ox}. Kinetic experiments were performed under pseudo-first-order conditions in which the Fd_{ox} concentration is present in large excess over the concentration of dRfH$^{\bullet}$ generated by the laser flash (<1 μM). Samples containing 0.1 mM dRf and 1 mM EDTA in 4 mM potassium phosphate buffer (pH 7.0) were deaerated by bubbling for 1 h with H_2O-saturated Ar gas. Microliter volumes of concentrated protein solution were then introduced into the sample contained in a 1-cm path length cuvette through a rubber septum. Ar gas was blown over the sample surface to remove traces of added O_2. Ionic strength was adjusted using aliquots of 5 M NaCl. Generally 4−10 kinetic traces were averaged. Kinetic traces were analyzed using a computer fitting routine (Kinfit, Olis, Bogart, GA).

Circular Dichroism. Circular dichroism measurements were made using an Aviv model 62A DS circular dichroism spectrometer (Aviv Associates, Lakewood, NJ). Protein concentrations were 5 μM in 10 mM Tris buffer (pH 7.3) for measurements in the 250−550-nm range and 1 μM in H_2O in the 190−250-nm range. Four spectra were averaged. The temperature of the sample was 25 ± 0.5 °C.

Dissociation Constants. Dissociation constants (K_d) for the complex formed between wt Fd_{ox} and the E139K FNR_{ox} mutant were determined spectrophotometrically using split-cell cuvettes as described previously (*41*). As mentioned above, K_d values for the transient Fd_{red}−FNR_{ox} complex were determined by fitting the kinetic data to the exact solution of the differential equation describing the reaction (*14*, *15*) depicted in eq 2.

Reduction Potentials. On the basis of the concentration of E139K required to completely reoxidize Fd_{red} at $\mu = 12$ mM (measured at 507 nm), relative to the concentration of wt FNR required to reoxidixe Fd_{red}, it is estimated that the one-electron reduction potential of oxidized E139K is decreased to a very slight extent relative to wt FNR. Such a small change in reduction potential cannot be the cause of the large decrease in et reactivity observed for this mutant (see below). The reduction potentials of E139K at $\mu = 100$ mM and of the E139D and E139Q mutants at both ionic strengths are estimated to be essentially identical to wt FNR.

Electrostatic Surface Potential Maps. Electrostatic potentials of Fd and FNR were calculated using the software package DELPHI (Molecular Simulations, Inc., San Diego, CA), with an ionic strength of 12 mM. Mapping of the electrostatic potential onto the surface of the protein was performed using GRASP (*42*), with a potential range of −15 to + 15 kT. Coordinates for the crystal structure of FNR determined by Serre et al. (*8*) were obtained from the Brookhaven Protein Data Bank (file code 1QUE). Coordinates of the crystal structure of Fd determined by Rypniewski et al. (*6*) were also obtained from the Brookhaven Protein Data Bank (file code 1FXA). The structure of the E139K FNR mutant was generated by replacing the amino acid using Insight II (Molecular Simulations, Inc.).

RESULTS

Transient decay curves (monitoring FNR reduction to the semiquinone state at 600 nm) for the reduction of FNR_{ox} by Fd_{red} are shown in Figure 2 for wt FNR and the E139D, E139Q, and E139K mutants at comparable concentrations at 12 mM ionic strength. At this low ionic strength, it is apparent (see k_{obs} values given in legend to Figure 2) that the E139K charge-reversal mutant is quite impaired in its et interaction with Fd_{red} and that the E139Q charge neutralization mutant is also significantly impaired, although to a lesser extent. In contrast, E139D under these conditions is even faster than wt in its reactivity. These relative reactivities at low μ are reflected in the ionic strength dependency curves shown in Figure 3. Transients observed at 507 nm (data not shown), a wavelength that monitors Fd reduction and reoxidation, yield rate constants that are the same, within experimental error, as those obained at 600 nm. It is important to note that the experiments shown in Figure 2 were performed using 15 μM FNR and that the experiments

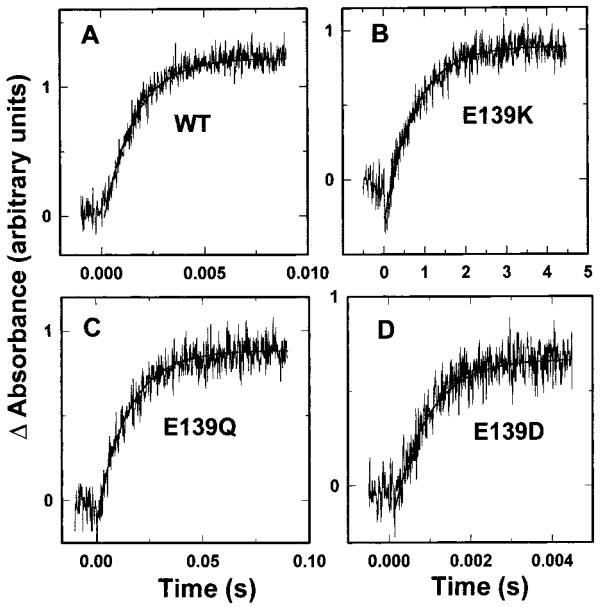

FIGURE 2: Transient decay curves showing the reduction of wt and mutant FNRs by reduced Fd. Deaerated solutions contained 15 μM FNR and 40 μM Fd in 4 mM potassium phosphate buffer (pH 7.0), containing 1 mM EDTA and 0.1 mM 5-deazariboflavin. The ionic strength was 12 mM, and the monitoring wavelength was 600 nm. Solid lines are single-exponential fits to the data; the rate constants obtained for these kinetic curves are 690 $\pm$ 20 s^{-1} for wt (panel A), 1.4 $\pm$ 0.4 s^{-1} for E139K (panel B), 70 $\pm$ 4 s^{-1} for E139Q (panel C), and 1200 $\pm$ 100 s^{-1} for E139D (panel D).

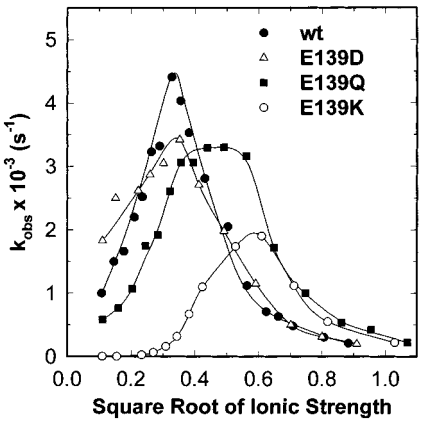

FIGURE 3: Ionic strength dependence of k_{obs} for the reduction of wt, E139D, E139Q, and E139K FNR by reduced Fd. Solutions contained 30 μM FNR and 40 μM wt Fd, except for the E139K experiment, which contained 15 μM FNR and 40 μM wt Fd (to minimize complications caused by direct reduction of FNR). All other conditions were the same as in Figure 2. The ionic strength was adjusted using aliquots of 5 M NaCl. Error limits are comparable to those in Figures 4−6.

shown in Figure 3 were performed using 30 μM FNR (except for the E139K experiment). The apparent discrepancy in reactivity for the E139Q mutant relative to wt FNR in these figures is due to the nonlinearity in k_{obs} observed for this mutant in going from 15 to 30 μM FNR (see below).

wt FNR. As previously shown (*43*), the dependence of k_{obs} on wt FNR concentration at μ = 12 mM (Figure 4) is predominantly linear at low FNR concentrations ($\leq$30 μM). However, a slight upward curvature is observed at higher FNR concentrations. At μ = 100 mM, saturation kinetics are obtained (Figure 4; *43*) as expected for the two-step mechanism depicted in eq 2. The values of k_{et} and K_d

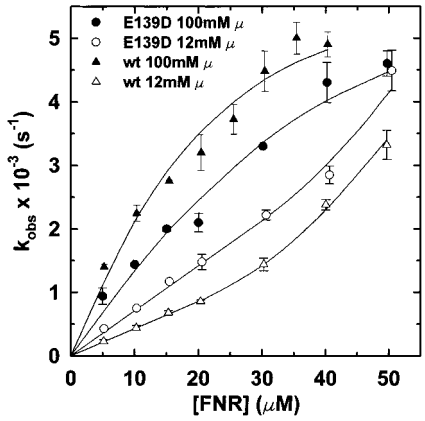

FIGURE 4: Dependence of k_{obs} on the concentrations of wt and E139D FNR at 12 and 100 mM ionic strengths. FNR was titrated into solutions containing 40 μM wt Fd. The ionic strength was adjusted using aliquots of 5 M NaCl. Other conditions were as in Figure 2. Data at μ = 100 mM for wt Fd are taken from ref *43*.

Table 1: Kinetic Parameters for Electron Transfer Interaction of wt and Mutant FNRs with wt Fd at Various Ionic Strengths[a]

FNR	μ (mM)	k_{et} (s^{-1})	K_d (μM)
wt	100	6200 $\pm$ 400[b]	9.3 $\pm$ 0.7[b]
	200	8100 $\pm$ 600	16.6 $\pm$ 1.2
E139K	200	2900 $\pm$ 100	12.8 $\pm$ 0.5
E139D	100	7100 $\pm$ 800	20.0 $\pm$ 2.2
E139Q	200	6400 $\pm$ 400	15.3 $\pm$ 0.9

[a] Deaerated solutions contained 100 μM 5-deazariboflavin and 1 mM EDTA in 4 mM potassium phosphate buffer, pH 7.0. Fd was titrated into 40 μM FNR. The ionic strength was adjusted using aliquots of 5 M NaCl. The monitoring wavelength was 600 nm. [b] Data taken from ref *43*.

Table 2: Binding of Oxidized wt and Mutant FNRs to Oxidized wt Fd at Various Ionic Strengths[a]

FNR	μ (mM)	K_d (μM)
wt	12	0.3 $\pm$ 0.1[b]
	100	3.3 $\pm$ 0.6[b]
E139K	12	0.8 $\pm$ 0.3
	100	2.7 $\pm$ 0.7
	200	7.3 $\pm$ 0.7
E139D	12	4.2 $\pm$ 0.9
	100	8.0 $\pm$ 0.2

[a] Solutions contained 1 mM EDTA in 4 mM potassium phosphate buffer, pH 7.0. Fd was titrated into 40 μM FNR. Aliquots of 5 M NaCl were used to adjust μ to 100 mM when necessary. [b] Data taken from ref *43*.

obtained from the latter kinetic data are 6200 s^{-1} and 9.3 μM (Table 1). Saturation kinetics were also obtained at μ = 200 mM (data not shown), and the values of k_{et} and K_d obtained from these measurements are also given in Table 1. The values of K_d for the complex formed between the oxidized wt proteins were measured at μ = 12 and 100 mM and were found to be 0.3 $\pm$ 0.1 and 3.3 $\pm$ 0.6 μM, respectively (Table 2; *43*).

Previously obtained data (*43*) for the dependence of k_{obs} on μ for the reduction of wt FNR_{ox} by Fd $_{red}$ are shown in Figure 3. The increase in rate constant as μ is increased in the low μ region is ascribed to the "loosening" of nonproductive et complexes that are held together by electrostatic forces (*12*, *43*). This allows the attainment of more reactive orientations of the proteins within the complexes leading to more rapid et. The decrease in k_{obs} at higher ionic strengths

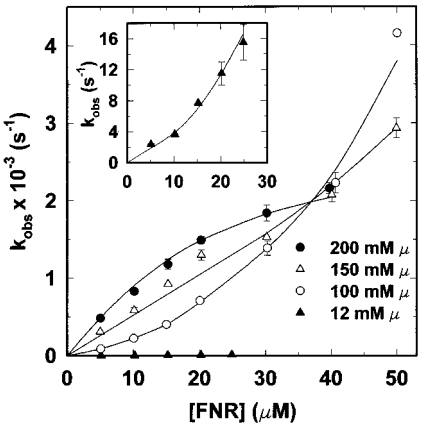

FIGURE 5: Dependence of k_{obs} on the concentrations of E139K FNR at various ionic strengths. FNR was titrated into solutions containing 40 μM wt Fd. The ionic strength was adjusted using aliquots of 5 M NaCl. Other conditions were as in Figure 2. Inset: 12 mM ionic strength data plotted on an expanded scale.

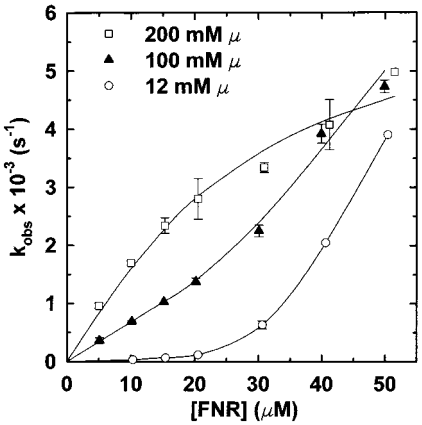

FIGURE 6: Dependence of k_{obs} on the concentrations of E139Q at 12, 100, and 200 mM ionic strengths. FNR was titrated into solutions containing 40 μM wt Fd. The ionic strength was adjusted using aliquots of 5 M NaCl. Other conditions were as in Figure 2.

is ascribed to screening of the net oppositely charged proteins by salt ions, thereby diminishing long-range electrostatic attractive forces (*43*).

E139K FNR. The dependence of k_{obs} on FNR concentration for the E139K charge-reversal mutant at various values of μ is shown in Figure 5. At $\mu = 12$, 100, and 150 mM, this dependence shows *upward curvature*, unlike the saturation kinetics expected for the mechanism depicted in eq 2. It is clear from these results that E139K is severely hindered in et at $\mu = 12$ mM; even at the highest FNR concentration used, the value of k_{obs} is less than 20 s^{-1} (Figure 5, inset). Increasing μ to 100−150 mM increases k_{obs} very significantly, diminishes the degree of upward curvature, and shifts the onset of curvature to higher FNR concentrations. The expected saturation kinetics are observed for the E139K reaction at $\mu = 200$ mM (Figure 5).

For this mutant, the maximum in the ionic strength dependence of k_{obs} (Figure 3) is clearly shifted to a higher value of μ ($\mu \approx 0.375$ mM, corresponding to $\mu^{1/2} \approx 0.6$ $mM^{1/2}$ in Figure 3), indicating that considerably higher salt concentrations compared to wt FNR are required to allow the attainment of the most productive mutual orientation. Below about $\mu = 120$ mM ($\mu^{1/2} \approx 0.35$ $mM^{1/2}$), the values of k_{obs} are extremely small. From the E139K concentration dependence of k_{obs} at $\mu = 200$ mM (Figure 5), the values of the kinetic constants, k_{et} and K_d (for the transient et complex), are 2900 ± 100 s^{-1} and 12.8 ± 0.5 μM, respectively (Table 1). This value for k_{et} is 35% as large as the value obtained for wt FNR (8100 ± 600 s^{-1}; Table 1) at this ionic strength, and the K_d is not too different from that determined for wt FNR (16.6 ± 1.2 μM; Table 1). The K_d value determined for oxidized E139K with Fd_{ox} at $\mu = 12$ mM (0.8 ± 0.3 μM; Table 2) is only 2−3 times larger than for wt FNR (0.3 ± 0.1 μM; Table 2) and is equivalent to wt FNR at $\mu = 100$ mM (2.7 ± 0.7 μM for E139K vs 3.3 ± 0.6 μM for wt FNR; Table 2). Thus, the effect of low ionic strength on dramatically decreasing the et rate constant for the mutant is not due to changes in the complex formation constants for either the oxidized or the reduced proteins or to the intrinsic reactivity of the E139K mutant (note that the limiting k_{et} value for this mutant is still quite rapid at 2900 ± 100 s^{-1}; Table 1). It should also be noted in this context that the circular dichroism spectra (data not shown) of the E139K mutant protein in both the visible and UV regions are essentially identical to those obtained for wt FNR, indicating that no gross structural perturbations arose as a result of the mutation. Thus, differences in reactivity are not attributable to major structural changes caused by the mutation. It is expected, however, that a charge-reversal in the predominantly negatively charged area close to E139 (Figure 1) might cause electrostatic surface potential changes that could change the mutual orientation of the proteins in the transient complex.

E139Q FNR. The maximum in the ionic strength dependence of k_{obs} for the E139Q charge-neutralization mutant (Figure 3) is also shifted to a higher μ value than for wt FNR (about 210 mM; $\mu^{1/2} \approx 0.45$ $mM^{1/2}$), although appreciably less so than for the E139K mutant. This again indicates that more salt is required to allow the attainment of the most optimal conformation for et for this pair of proteins as compared to the wt proteins. Assuming that E139K interacts with negative charges on Fd, it is not unexpected that the peak for E139Q occurs at a lower μ value than E139K since attractive interactions experienced by the E139K mutant that result in highly nonproductive orientations are not present in the E139Q mutant. Alternatively, any repulsive interactions between E139K and the positive charges on the Fd surface that contribute to the mutual orientation of the proteins in the complex would be decreased for the E139Q mutant. In addition, repulsive interactions occurring between E139 in wt FNR and the net negatively charged Fd surface are lost as a consequence of the E139Q mutation. This is very likely an additional factor in the broadening of the ionic strength dependency curve for E139Q (Figure 3).

Like the E139K mutant, the dependence of k_{obs} on E139Q concentration shows upward curvature at $\mu = 12$ and 100 mM, although this is only evident at significantly higher FNR (>20 μM) concentrations than with the E139K mutant (Figure 6). As with the E139K mutant, saturation kinetics were observed at $\mu = 200$ mM for E139Q (Figure 6). From these data, values of 6400 ± 400 s^{-1} and 15.3 ± 0.9 μM were obtained for K_d and k_{et}, respectively (Table 1). Note that these values are comparable to those of wt FNR at high values of μ (Table 1) and that the k_{et} value is significantly larger than that for E139K (2900 ± 100 s^{-1}). Again, the

circular dichroism spectra (data not shown) of the E139Q mutant protein are essentially identical to those obtained for wt FNR, indicating that no gross structural perturbations resulted from the mutation. Thus, any differences in reactivity cannot be attributed to structural alterations caused by the mutation. Although neutralization of the negative charge at E139 is expected to alter the electrostatic surface potential in this area of the molecular surface (Figure 1, lower) and thus would be expected to change the mutual orientation of the proteins in the transient complex, this should not occur to the same extent as for a charge reversal mutation.

E139D FNR. The E139D charge-conservation mutant reacts with Fd in a manner very similar to wt at all values of μ (Figure 3). Although the value of the maximal k_{obs} value attained in the ionic strength dependence experiment (Figure 3) is somewhat smaller than that obtained with wt FNR, the ionic strength at which this maximum is realized is the same as for wt FNR. Furthermore, k_{obs} at $\mu = 12$ mM in the ionic strength dependency curve (Figure 3) is somewhat larger for E139D as compared to wt. This latter observation is consistent with the k_{obs} dependencies on E139D and wt FNR concentrations at $\mu = 12$ mM (Figure 4). As in the case of wt FNR and the other mutants at $\mu = 12$ mM, upward curvature is also observed, although at appreciably higher concentrations of E139D than for the K and Q mutants. Saturation kinetics are observed at $\mu = 100$ mM for E139D (Figure 4), and the kinetic constants obtained from these data are given in Table 1. The value of k_{et} (7100 ± 800 s^{-1}; Table 1) is similar to the wt value (6200 ± 400 s^{-1}), and the value of K_d (20.0 ± 2.2 FM; Table 1) is about a factor of 2 larger than the value determined for wt FNR (9.3 ± 0.7 FM) at this value of μ. The values of K_d determined for the oxidized proteins at $\mu = 12$ and 100 mM (4.2 ± 0.9 and 8.0 ± 0.2 μM, respectively) are given in Table 2. At both values of μ, K_d for the oxidized proteins is larger for the E139D mutant than for wt FNR, as was observed for the transient complex at $\mu = 100$ mM (Table 1). A charge conservation mutation at E139 would be expected to have minimal effects on the mutual orientation of the proteins in the transient complex, which seems to be the case based on the kinetic behavior observed for the E139D mutant.

DISCUSSION AND CONCLUSIONS

As described above, the upward curvature in the FNR concentration dependence observed at low ionic strengths and at higher FNR concentrations is especially exaggerated in the E139K mutant and to a lesser extent in the E139Q mutant and is found to a still smaller extent in E139D and wt FNRs. This behavior can be explained by the mechanism depicted in Figure 7. Here it is assumed that binding of photochemically reduced Fd (pathway A) to FNR_{ox} at low ionic strengths produces a $Fd_{red}-FNR_{ox}$ complex in which the mutual orientation of the proteins is not optimal for et, resulting in a slow intracomplex et process (a particularly poor mutual orientation is depicted for the complex shown in Figure 7, with the et cofactors being situated at the furthest possible distance from one another). The degree of nonoptimal orientation varies with the FNR, being most severe in the E139K mutant and progressively less so in the E139Q, E139D, and wt proteins. As shown in Figure 7, reduction of Fd_{ox} in a preformed complex between oxidized proteins (pathway B) results in the same nonoptimal slowly reacting

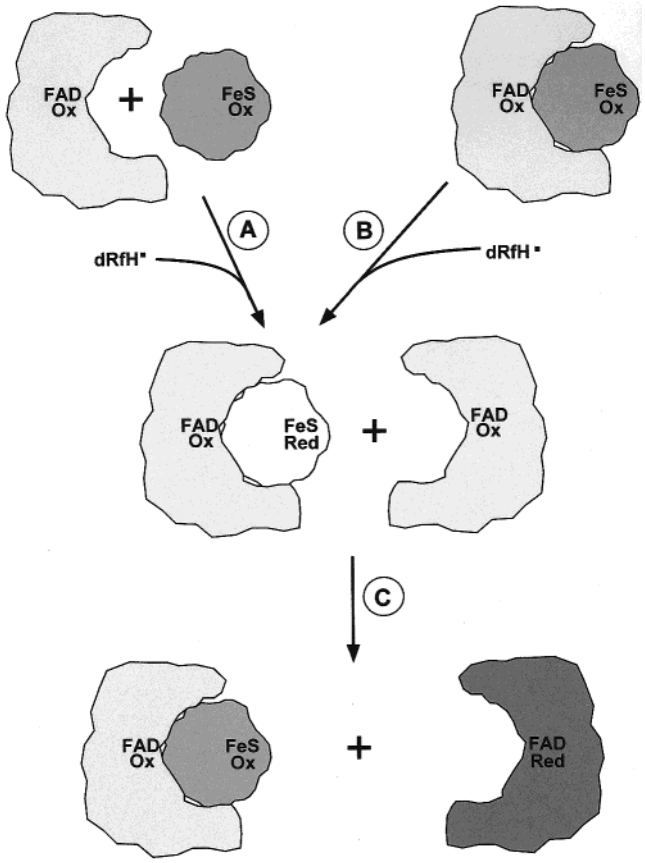

FIGURE 7: Mechanism of interaction of FNR with Fd at low ionic strengths. The Fd−FNR complexes shown are schematic representations of nonoptimal complexes, with the Fe−S center of Fd occupying the furthest possible position from the FAD of FNR. 5-Deazariboflavin semiquinone either reduces free Fd_{ox} (pathway A), which then binds to FNR_{ox} or reduces Fd in a preformed $Fd_{ox}-FNR_{ox}$ complex (pathway B). In either case, the resulting $Fd_{red}-FNR_{ox}$ complex is nonoptimal and reacts slowly. As the concentration of FNR increases, a collisional interaction occurs whereby free FNR_{ox} oxidizes the exposed Fe−S center of the reduced Fd in the complex (pathway C).

complex. As the total concentration of FNR_{ox} is increased in the reaction mixture, the reduced complex is able to react with free FNR_{ox} via a collisional interaction resulting in oxidation of the Fd_{red} in the complex and formation of FNR_{red} (pathway C). In all cases, but especially in the E139K mutant, this reaction proceeds more rapidly than the intracomplex reaction as the FNR concentration is increased. This results in upward curvature of the k_{obs} vs [FNR] curves at the higher concentrations of FNR. The degree of reactivity of the complex determines the FNR concentration and the ionic strength range at which this nonlinear behavior is observed. Thus, the E139K charge-reversal mutation results in the least favorable orientation of the proteins and the most nonreactive complex with Fd. The E139Q mutation allows a more reactive, yet still significantly nonoptimal complex. At the higher ionic strengths where saturation kinetics are observed, the proteins can apparently bind such that the [2Fe-2S] center of Fd and the FAD of FNR can "communicate" effectively, i.e., nonproductive complex formation is minimal or nonexistent.

Inasmuch as the interaction between Fd and FNR is known to be predominantly electrostatic in nature, it is instructive to examine the electrostatic surface potential maps of Fd and

FNR shown in Figure 1. It is important to note that the FNR map is based on an X-ray structure of the protein that includes the seven N-terminal residues that are typically proteolytically removed during the preparation of the native FNR.

The electrostatic surfaces of these proteins can be readily divided into several distinct neutral or charged regions. The front face of Fd, shown in the upper left panel of Figure 1, contains a "bulge" (referred to below as the FeS bulge) that corresponds to the closest distance between the [2Fe-2S] center and the protein surface, and is seen to be electrostatically neutral under the conditions of the calculation (±15 kT and 12 mM ionic strength). Immediately above the FeS bulge is a region of negative charge generated by E94 and E95. E94, the closer of the two glutamates to the FeS center, has been shown (*10*) to be absolutely essential for the et interaction of Fd with FNR, whereas mutations at E95 have little or no effect. Immediately below and to the right of the FeS bulge is a positive charge due to R42, which has also been shown not to be important in the interaction with FNR (*10*). The majority of the acidic residues in Fd are located in two regions that are relatively far from the FeS bulge. A large acidic patch, consisting of D67, D68, D69, and E72, can be seen to the upper left of the FeS bulge (Figure 1, upper left panel) as a large negatively charged projection. This region has been shown (*13*) to be important (although not crucial) for the et reaction between the two proteins. The majority of the negative charge in Fd is located below the FeS bulge (Figure 1, upper left panel). This negative patch extends around to the "backside" surface of the protein (Figure 1, upper right panel, shows a view rotated 180° about the *y*-axis) and is comprised of eight acidic residues (D22, D23, E24, D28, E31, E32, D59, and D62). Of these, D28, E31, and E32 have been shown to be relatively unimportant for the et interaction with FNR (unpublished data); the other residues have not been evaluated. The backside view of Fd also shows three positively charged residues (K4, K15, and K52) that are located around the periphery of a region that otherwise is electrostatically neutral. The possible importance of these for et with FNR has also not been tested.

It is likely that changes in the electrostatic surface potential of the FNR, which alter the precise orientations of the proteins in the complex, are the cause of the lowered reactivity of E139K and E139Q at low μ. As shown in Figure 1 (lower left panel), the partially exposed dimethylbenzene ring of the FAD is surrounded by a ring of positively charged residues, which in turn surrounds a negatively charged surface depression containing E139. A charge-reversal mutation in this negatively charged residue might be expected to have a significant effect on the geometry of the electrostatically interacting protein surfaces. As is shown in Figure 1 (lower right panel), this charge-reversal not only places a positive charge on the residue itself but also neutralizes a significant portion of the negative charge located in the depression in the FNR surface. It is reasonable to expect that this will significanty alter repulsive interactions between the two proteins, which undoubtedly participate in the complex formation process. In this regard, it has previously been pointed out in the case of the interaction between the [3Fe-4S] FdI from *Azotobacter vinelandii* and NADPH-ferredoxin reductase (FPR) that "both attractive and repulsive forces appear to play a role in orienting FdI and FPR for interaction" (*44*). The present results indicate that a similar situation is also operative in the interaction between the *Anabaena* proteins. It is also possible that, in the present system, the positive charges located on the backside of Fd (Figure 1, upper right panel) are involved in the overall docking process. This requires further study. It is clearly evident, however, that the E139Q charge-neutralization mutation lessens repulsive interactions between E139 and the Fd surface, which are involved in achieving proper orientations of the proteins leading to et. As previously stated, this loss of electrostatic repulsion contributes to the broadened ionic strength dependency curve observed for this mutant (Figure 3).

The fact that at $\mu = 12$ mM, the value K_d for E139K with Fd in the oxidized form (Table 2) is quite similar to that found for the wt proteins is striking in light of the large difference in reactivity at this low value of μ. Even at $\mu =$ 100 mM, the binding constant for the complex of E139K and wt Fd is the same as that measured for the wt proteins (Table 2), although the reactivities are still quite different (Figure 3). These findings support the conclusion that the mutual orientation between the proteins in the transient complex is the main factor affecting reactivity in these et protein complexes. This same conclusion was reached in an extensive study (*11*) that included thermodynamic and X-ray structural studies in addition to kinetic studies on a number of Fd mutants. Thus, it appears from our work that a unifying theme in protein−protein et, at least in the Fd/FNR protein system from *Anabaena*, is that it is this mutual orientation that is the principal factor governing et reactivity.

REFERENCES

1. Alam, J., Whitaker, R. A., Krogman, D. W., and Curtis, S. E. (1986) *J. Bacteriol. 168*, 1265−1271.
2. Böhme, H., and Haselkorn, R. (1989) *Plant Mol. Biol. 12*, 667−672.
3. Fillat, M. F., Borrias, W. E., and Weisbeek, P. J. (1990) in *Flavins and Flavoproteins 1990* (Curti, B., Ronchi, S., and Zanetti, G., Eds.) pp 445−448, Walter de Gruyter and Co., Berlin.
4. Fillat, M. F., Pacheco, M. L., Peleato, M. L., and Gómez-Moreno, C. (1994) in *Flavins and Flavoproteins 1993* (Yagi, K., Ed.) pp 447−450, Walter de Gruyter and Co., Berlin.
5. Gómez-Moreno, C., Martinez-Júlvez, M., Fillat, M. F., Hurley, J. K., and Tollin G. (1995) in *Photosynthesis: from Light to Biosphere* (Mathis, P., Ed.) Vol. II, Academic, Dordrecht, The Netherlands.
6. Rypniewski, W. R., Breiter, D. R., Benning, M. M., Wesenberg, G., Oh, B.-H., Markley, J. L., Rayment, I., and Holden, H. M. (1991) *Biochemistry 30*, 4126−4131.
7. Holden, H. M., Jacobson, B. L., Hurley, J. K., Tollin, G., Oh, B.-H., Skjeldahl, L., Chae, Y. K., Cheng, H., Xia, B., and Markley, J. L. (1994) *J. Bioenerg. Biomembr. 26*, 67−88.
8. Serre, L., Vellieux, F. M. D., Medina, M., Gómez-Moreno, C., Fontecilla-Camps, J. C., and Frey, M. (1996) *J. Mol. Biol. 263*, 20−39.
9. Walker, M. C., Pueyo, J. J., Navarro, J. A., Gómez-Moreno, C., and Tollin, G. (1991) *Arch. Biochem. Biophys. 287*, 351−358.
10. Hurley, J. K., Salamon, Z., Meyer, T. E., Fitch, J. C., Cusanovich, M. A., Markley, J. L., Cheng, H., Xia, B., Chae, Y. K., Medina, M., Gómez-Moreno, C., and Tollin, G. (1993) *Biochemistry 32*, 9346−9354.
11. Hurley, J. K., Weber-Main, A. M., Stankovich, M. T., Benning, M. M., Thoden, J. B., Vanhooke, J. L., Holden, H. M., Chae, Y. K., Xia, B., Cheng, H., Markley, J. L., Martinez-Júlvez,

M., Gómez-Moreno, C., Schmeits, J. L., and Tollin, G. (1997) *Biochemistry 36*, 11100−11117.
12. Hurley, J. K., Fillat, M., Gómez-Moreno, C., and Tollin, G. (1995) *Biochimie 77*, 539−548.
13. Hurley, J. K., Schmeits, J. L., Genzor, C., Gómez-Moreno, C., and Tollin, G. (1996) *Arch. Biochem. Biophys. 333*, 243−250.
14. Simondsen, R. P., Weber, P. C., Salemme, F. R., and Tollin, G. (1982) *Biochemistry 24*, 6366−6375.
15. Simondsen, R. P., and Tollin, G. (1983) *Biochemistry 22*, 3008−3016.
16. Hurley, J. K., Cheng, H., Xia, B., Markley, J. L., Medina, M., Gómez-Moreno, C., and Tollin, G. (1993) *J. Am. Chem. Soc*. *115*, 11698−11701.
17. Hurley, J. K., Medina, M., Gómez-Moreno, C., and Tollin, G. (1994) *Arch. Biochem. Biophys*. *312*, 480−486.
18. Holden, H. M., Jacobson, B. L., Hurley, J. K., Tollin, G., Oh, B.-H., Skjeldahl, L., Chae, Y. K., Cheng, H., Xia, B., and Markley, J. L. (1994) *J. Bioenerg. Biomembr. 26*, 67−88.
19. Morales, R., Chron, M.-H., Hudry-Clergeon, G., Pétillot, Y., Norager, S., Medina, M., and Frey, M. (1999) *Biochemistry 38*, 15764−15773.
20. Martínez-Júlvez, M., Medina, M., Hurley, J. K., Hafezi, R., Brodie, T. B., Tollin, G., and Gómez-Moreno, C. (1998) *Biochemistry 37*, 13604−13613.
21. Hurley, J. K., Hazzard, J. T., Martínez-Júlvez, M., Medina, M., Gómez-Moreno, C., and Tollin, G. (1999) *Protein Sci. 8*, 1614−1622.
22. Schmitz, S., Martínez-Júlvez, M., Gómez-Moreno, C., and Böhme, H. (1998) *Biochim. Biophys. Acta 1363*, 85−93.
23. Medina, M., Martínez-Júlvez, M., Hurley, J. K., Tollin, G., and Gómez-Moreno, C. (1998) *Biochemistry 37*, 2715−2728.
24. Mayoral, T., Medina, M., Sanz-Aparicio, J., Gómez-Moreno, C., and Hermoso, J. (2000) *Proteins: Struct., Funct. Genet. 38*, 60−69.
25. Kang, C. H., Ferguson-Miller, S., and Margoliash, E. (1977) *Biochemistry 252*, 919−926.
26. Nuevo, M. R., Chu, H.-H., Vitello, L. B., and Erman, J. E. (1993) *J. Am. Chem. Soc. 115*, 5873−5874.
27. Mauk, M. R., Ferrer, J. C., and Mauk, A. G. (1994) *Biochemistry 33*, 12609−12614.
28. Zhou, J. S., Nocek, J. M., DeVan, M. L., and Hoffman, B. M. (1995) *Science 269*, 204−207.
29. Zhou, J. S., Tran, S. T., McLendon, G., and Hoffman, B. M. (1997) *J. Am. Chem. Soc. 119*, 269−277.
30. Gómez-Moreno, C., Martinez-Júlvez, M., Fillat, M. F., Hurley, J. K., and Tollin G. (1995) in *Photosynthesis: from Light to Biosphere* (Mathis, P., Ed.) Vol. II, Academic, Dordrecht, The Netherlands.
31. Pueyo, J. J., and Gómez-Moreno, C. (1991) *Prepr. Biochem. 21*, 191−204.
32. Böhme, H., and Haselkorn, R. (1989) *Plant Mol. Biol. 12*, 667−672.
33. Deng, W. P., and Nickoloff, J. A. (1992) *Anal. Biochem 200*, 81−88.
34. Ausubel, F. M., Brent, R., Kingston, R. E., Moore, D. D., Seidman, J. G., Smith, J. A., and Struhl, K., Eds. (1989) *Current Protocols in Molecular Biology*, John Wiley and Sons, New York.
35. Sambrook, J., Fritsch, E. F., and Maniatis, T. (1989) *Molecular Cloning, A Laboratory Manual*, Cold Spring Harbor Laboratory Press, Plainview, NY.
36. Przysiecki, C. T., Bhattacharyya, A. K., Tollin, G., and Cusanovich, M. A. (1985) *J. Biol. Chem. 260*, 1452−1458.
37. Bhattacharyya, A. K., Tollin, G., Davis, M., and Edmondson, D. E. (1983) *Biochemistry 22*, 5270−5279.
38. Tollin, G. (1995) *J. Bioenerg. Biomembr. 27*, 303−309.
39. Tollin, G., Hurley, J. K., Hazzard, J. T., and Meyer, T. (1993) *Biophys. Chem. 48*, 259−279.
40. Tollin, G., and Hazzard, J. T. (1991) *Arch. Biochem. Biophys. 287*, 1−7.
41. Sancho, J., and Gómez-Moreno, C. (1991) *Arch. Biochem. Biophys. 288*, 231−238.
42. Nicholls, A., Sharp, K., and Honig, B. (1991) *Proteins: Struct. Funct. Genet. 11*, 281−296.
43. Hurley, J. K., Fillat, M. F., Gómez-Moreno, C., and Tollin, G. (1996) *J. Am. Chem. Soc. 118*, 5526−5531.
44. Jung, Y.-S., Roberts, V. A., Stout, C. D., and Burgess, B. K. (1999) *J. Biol. Chem. 274*, 2978−2987.

BI001124R